

LOCAL ACTIVE CONTENT FINGERPRINTING: OPTIMAL SOLUTION UNDER LINEAR MODULATION

Dimche Kostadinov, Slava Voloshynovskiy, Maurits Diephuis and Taras Holotyak

Computer Science Department, University of Geneva, 7 Route de Drize, Carouge GE, Switzerland

ABSTRACT

This paper presents an analysis on Active Content Fingerprint (aCFP) for local (patch based) image descriptors. A generalization is proposed, the reduction of the aCFP with linear modulation to a constrained projection problem is shown and the optimal solution is given. The constrained projection problem addresses the linear modulation by a constraint on the properties of the resulting local descriptor. A computer simulation using local image patches, extracted from publicly available data sets is provided, demonstrating the advantages under several signal processing distortions.

Index Terms— active content fingerprint, modulation, local descriptor, robustness and constrained projection

1. INTRODUCTION

Active Content Fingerprinting (aCFP) has emerged as a synergy between digital watermarking (DWM) and passive content fingerprinting (pCFP) [1]. This alternative approach covers a range of applications in the case when content modulation is appropriate, prior to content distribution/reproduction. The advantages are related to a number of applications, including content authentication, identification and recognition.

Recently, theoretically it was demonstrated that the identification capacity of aCFP [2] under additive white Gaussian channel distortions and ℓ_2 -norm embedding distortion is considerably higher to those of DWM and pCFP. Interestingly, the optimal modulation of aCFP produces the correlated modulation to the content in contrast to the optimal modulation of DWM where the watermark is independent to the host. Several scalar and vector modulation schemes for the aCFP have been proposed [3, 4] and have been tested on synthetic signals and collections of images. Despite of the attractive theoretical properties of aCFP, the practical implementation of aCFP modulation with an acceptable complexity, capable to jointly withstand *signal processing* distortions such as additive white Gaussian noise (AWGN), lossy JPEG compression, histogram modifications and *geometrical distortions* (affine and projective transforms) remains an open and challenging problem.

On the other hand in recent years, local, i.e., *patch-based*, compact, geometrically robust, binary descriptors such as

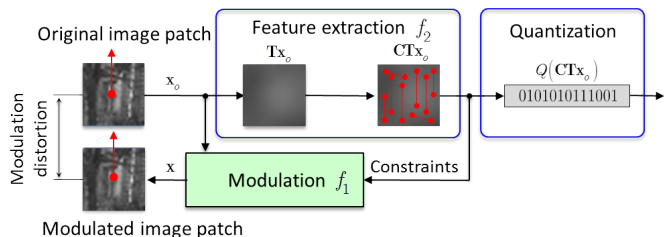


Fig. 1. Local aCFP framework

SIFT [5], BRIEF [6], BRISK [7], ORB[8] and the family of LBP [9] became a popular tool in image processing, computer vision and machine learning. These local descriptors are also considered as a form of local pCFP.

However, up to our best knowledge, there is no prior work on the modulation of local descriptors in the scope of aCFP or DWM. Therefore, in this paper, we investigate in the direction towards the modulation on the local image descriptor and focus on the robustness to several signal processing distortions. Along this way, we propose aCFP with a linear modulation subject to convex constraint on the properties of the resulting local descriptors.

The paper is organized as follows. In Section 2 the problem is introduced, a short description of the local pCFP is given and the local aCFP modulation is presented. In Section 3 the main result is stated. Section 4 is devoted to computer simulation and Section 5 concludes the paper.

2. LOCAL (PATCH BASED) LINEAR MODULATION

The proposed aCFP framework consists of modulation, prior to the content reproduction and descriptor extraction that includes feature mapping and quantization. The scheme of the local aCFP framework is shown in Figure 1.

The core idea behind the aCFP modulation [3] is based on the observation that the magnitude of the feature coefficients before the quantization influences the probability of the bit error in the descriptor bits. The descriptor bit flipping is more likely for low magnitude coefficients. Therefore, it is natural to modify the original content by an appropriate modulation and to increase these magnitudes subject to some distortion constraint. Obviously, the modulation faces a trade-off

between two conflicting requirements of feature coefficient magnitude increase for the probability of bit error reduction and the modulation distortion. Fortunately, the low magnitude coefficient are concentrated near zero and are easily affected by a low distortion modulation.

Note that the local aCFP scheme is applicable also in the context of global image description. Nevertheless, considering either global or local image description, here a novel approach to aCFP is presented, alternatively to the scheme considered in [4].

2.1. Local descriptor extraction (pCFP): no patch modulation

Given an original image, around a local key point, local image patch $\mathbf{x}_o \in \mathbb{R}^{N \times 1}$ is extracted. Usually the patch extraction is performed according to the patch orientation defined for example by a patch gradient (shown in red in Figure 1).

Given a patch \mathbf{x}_o in the most general case, the local features are extracted using a mapping function $f_2 : \mathbb{R}^{N \times 1} \rightarrow \mathbb{R}^{L \times 1}$, where L is the length of the descriptor. Consider a linear function $f_2(\mathbf{x}_o) = \mathbf{A}\mathbf{x}_o$, then $\mathbf{A} \in \mathbb{R}^{L \times N}$ is a map (note that the map is either predefined, data independent and analytic or learned, data dependent and adaptive). The mapping, followed by a quantization $Q(\cdot)$ results in the local descriptor $\mathbf{b}_x = Q(\mathbf{A}\mathbf{x}_o)$. The differences between the existing classes of local descriptors are determined by the defined mapping $f_2(\cdot)$ and the type of the quantization $Q(\cdot)$.

2.2. Local aCFP: patch modulation

The analysis here is focused on the optimal solution under linear maps and scalar quantizers used in such descriptors as ORB and LBP.

Linear modulation. We consider linear aCFP modulation $f_1 : \mathbb{R}^{N \times 1} \rightarrow \mathbb{R}^{N \times 1}$, $f_1(\mathbf{x}_o) = \mathbf{Z}\mathbf{x}_o$, $\mathbf{Z} \in \mathbb{R}^{N \times N}$ to local image patches \mathbf{x}_o .

Linear feature extraction. The considered feature extraction is linear $f_2(\mathbf{x}_o) = \mathbf{A}\mathbf{x}_o$, defined as $\mathbf{A} = \mathbf{C}\mathbf{T}$. The matrix $\mathbf{T} \in \mathbb{R}^{M \times N}$ represents a linear transform, examples include low pass filter, DCT, FFT, WDT, random projections and others that typically are used by most of the known local descriptors for decorrelation and "robustification" of the features. The matrix $\mathbf{C} \in \{-1, 0, +1\}^{L \times M}$ is a m -wise (pairwise, triplewise, etc.) constraint matrix denoting a geometrical configuration of pixel interaction contributing to a feature extraction to be quantized.

Binary quantization. The quantization is defined as $\mathbf{b}_y = Q(\mathbf{A}\mathbf{x}_o + \mathbf{A}\mathbf{x}_e + \mathbf{A}\mathbf{x}_n)$, where \mathbf{x}_n and \mathbf{x}_e are the modulation and the signal processing distortions respectively and $Q(a) = \text{sign}(a) = 1$, if $a \geq 0$ and 0, otherwise.

3. MAIN RESULT

The aCFP modulation set-up is addressed by the analysis of the generalized problem formulation that reduces to a constrained projection problem.

3.1. Generalization

Proposition 1: *The generalized aCFP is a solution to a problem of functions estimation:*

$$\min_{f_1, f_2} \varphi(f_1(\mathbf{x}_o), \mathbf{x}_o) + \lambda_1 \psi(f_2(f_1(\mathbf{x}_o)), \tau), \quad (1)$$

where the first mapping function f_1 is the aCFP modulation that modifies the local data in the original domain and $\varphi(\cdot)$ is a function that penalizes the modulation distortions in the original data domain. The second mapping function f_2 transforms the modified local data $f_1(\mathbf{x}_o)$ and $\psi(\cdot)$ is a function that penalizes non-robust feature components. The modulation level is denoted as τ and λ_1 is Lagrangian variable.

3.2. Reduction to a constrained projection problem

Consider the following constraints:

1. *The first map $f_1(\mathbf{x}_o) = \mathbf{Z}\mathbf{x}_o$ is linear, the second $f_2(f_1(\mathbf{x}_o))$ is linear and parametrized by \mathbf{Z} and \mathbf{A} respectively.*

2. *The functions $\psi(\cdot)$, $\varphi(\cdot)$ and \mathbf{A} are a priori defined. Let a transformation matrix be denoted as $\mathbf{T} \in \mathbb{R}^{M \times N}$ and a constraint matrix be denoted as $\mathbf{C} \in \{-1, 0, +1\}^{L \times M}$. Further let $\mathbf{A} = \mathbf{C}\mathbf{T}$, replace ψ by a constraint $\phi(\mathbf{Z}\mathbf{x}_o, \mathbf{A}) \geq_e \mathbf{0}$ and let $\varphi(\mathbf{Z}\mathbf{x}_o, \mathbf{x}_o) = \|\mathbf{Z}\mathbf{x}_o - \mathbf{x}_o\|_2^2$, where \geq_e means element-wise inequality and $\mathbf{0} \in \mathbb{R}^{L \times 1}$ is a zero vector.*

3. *The variable reduction is defined as $\mathbf{x} = \mathbf{Z}\mathbf{x}_o$ and let $\phi(\mathbf{x}, \mathbf{A}) = |\mathbf{A}\mathbf{x}| - \tau\mathbf{1}$, where $|\mathbf{A}\mathbf{x}|$ is an element-wise absolute value of the vector $\mathbf{A}\mathbf{x}$.*

Corollary 1: *Given the constraints 1, 2 and 3, aCFP with linear modulation reduces to a constrained projection problem:*

$$\begin{aligned} \hat{\mathbf{x}} &= \underset{\mathbf{x}}{\text{argmin}} \frac{1}{2} (\mathbf{x}_o - \mathbf{x})^T (\mathbf{x}_o - \mathbf{x}) \\ &\text{subject to} \\ &|\mathbf{C}\mathbf{T}\mathbf{x}| \geq_e \tau\mathbf{1}. \end{aligned} \quad (2)$$

The main result about the global optimal solution of (2) is stated by the following theorem.

Theorem 1: *If $\exists \mathbf{x}_e \in \mathbb{R}^N$ such that $\mathbf{A}\mathbf{x}_e = \mathbf{t}_e$, where $\mathbf{t}_e = (\text{sign}(\mathbf{A}\mathbf{x}_o) \odot \max\{\tau\mathbf{1} - |\mathbf{A}\mathbf{x}_o|, \mathbf{0}\})$, then the solution to (2) is $\mathbf{x} = \mathbf{x}_o + \mathbf{x}_e$, where \odot represents Hadamard (element-wise) product, moreover if \mathbf{A} is invertible or pseudo invertible then the closed form solution to (2) is $\mathbf{x} = \mathbf{x}_o + \mathbf{A}^\dagger \mathbf{t}_e$, where \mathbf{A}^\dagger is the pseudo inverse of \mathbf{A} .*

Proof: See Appendix A.

4. COMPUTER SIMULATIONS

A computer simulation is performed to demonstrate the advantages of the local aCFP scheme over pCFP, under several signal processing distortions, including AWGN, lossy JPEG compression and projective geometrical transform.

The UCID [10] image database was used to extract local image patches. The ORB detector [8] was run on all images, and $\sqrt{N} \times \sqrt{N}$ pixel patches, with $\sqrt{N} = 31$ were extracted around each detected feature point. The features were sorted

by scale-space, 30 patches were extracted from individual image. An average result for a total of 1000 image patches is provided.

Two scenarios: pCFP and aCFP are used in the computer simulation.

Two matrices $\mathbf{A}_0 \in \mathbb{R}^{L \times N}$ and $\mathbf{A}_1 \in \mathbb{R}^{L \times N}$ are used in the pCFP scenario. One matrix \mathbf{A}_1 is used in the aCFP scenario.

A square matrix $\mathbf{T}_i, i \in \{0, 1\}$ is used ($M = N$). The matrix $\mathbf{A}_0 = \mathbf{C}\mathbf{T}_0$ where $\mathbf{T}_0 \in \mathbb{R}^{N \times N}$ represents low pass filter with 11×11 window. The matrix $\mathbf{A}_1 = (\mathbf{U}\mathbf{I}_{L \times M}\mathbf{V}^T)^T$ where \mathbf{U}, \mathbf{V} are obtained by singular value decomposition (SVD) of $(\mathbf{C}\mathbf{T}_1)^T$. The matrix $\mathbf{T}_1 = \mathbf{R} [\mathbf{x}_o \mathbf{x}_o^T]^{-1} \in \mathbb{R}^{N \times N}$ and $\mathbf{R} \in \mathbb{R}^{N \times N}$ is random matrix, generated from uniform distribution with the support $[0, 1]$. The matrix \mathbf{A}_1^T is the closest orthogonal to $(\mathbf{C}\mathbf{T})^T$, satisfying $\mathbf{A}_1^T \mathbf{A}_1 = \mathbf{I}$ and easily invertible.

Three measured quantities are used for evaluation: 1) *the modulation distortion*, 2) *the probability of bit error* and 3) *the modulation level*.

The first is defined as $\text{DWR} = 10 \log_{10} \left(\frac{255^2}{\Delta} \right)$, $\Delta = \frac{1}{N} \|\mathbf{x} - \mathbf{x}_o\|_2^2$. The second is defined by the probability of correct bit $p_e = 1 - \frac{1}{L} \sum_{i=1}^L \mathcal{I}\{b_x(i) == b_y(i)\}$ with $L = 256$ bits, where \mathcal{I} is indicator function that returns 1 if the argument is true 0 otherwise. The modulation level mL is expressed in percentage $mL = \frac{K}{L} 100, 1 \leq K \leq L$ and it represents the fraction of coefficients s_o that are modified. At single modulation level, the modulation threshold τ is defined as $\tau = \max_{1 \leq i \leq K} |s(i)|$ where $s_o, |s_o(i)| \leq |s_o(j)|, 1 \leq i \leq j \leq L$ is the sorted $|\mathbf{t}_o|$ vector.

AWGN The results from a single patch was obtained as average of 100 AWGN realizations. Four different noise levels were used, defined in $\text{PSNR} = 10 \log_{10} \frac{255^2}{\sigma^2}$ are 0dB, 5dB, 10dB and 20dB. Two modulation levels (mL) were used 10 and 60. The results are shown in Table 2.

Lossy JPEG compression Three small JPEG quality factor (QF) levels 0, 5 and 10 were used. The modulation levels (mL) that were used are 10 and 30. The results are shown in Table 2.

Projective transform with lossy JPEG compression A projective transformation $\mathbf{P} \in \mathbb{R}^{3 \times 3}$ where $\mathbf{P}(1, :) = [1.0763, 0.0325, 0]$, $\mathbf{P}(2, :) = [0.0119, 1.09, 0]$ and $\mathbf{P}(3, :) = [-24.32, -70.37, 1]$ was used, followed by a lossy JPEG compression with QF=5. The modulation levels (mL) that were used are 10 and 60. The results are shown in Table 2.

Overall the aCFP scenario brings improvement, the results produced by \mathbf{A}_1 have consistently lower p_e than the results produced by \mathbf{A}_0 .

The aCFP under AWGN has the greatest reduction in p_e of 0.15 achieved at AWGN level of 0dB and modulation level $mL = 60$. Otherwise in the same aCFP scenario, when comparing the results produced by \mathbf{A}_1 to the ones produced by \mathbf{A}_1 with zero modulation, the greatest reduction is .08, achieved

		pCFP	
		p_e	
		\mathbf{A}_0	\mathbf{A}_1
AWGN	0dB	.26	.15
	5dB	.17	.12
	10dB	.11	.09
	20dB	.04	.03
QF	0	.05	0.3
	5	.03	.02
	10	.02	.01
Projective	QF=5	.08	.05

Table 1. The p_e using pCFP under varying AWGN noise, varying JPEG compression levels and projective transformation with QF level of 5.

at AWGN level of 10dB and modulation level $mL = 60$.

Considering the aCFP under the lossy JPEG compression, the modulation improves the results, even at small modulation level like $mL = 30$ and the greatest reduction in p_e is .05, achieved at QF=0.

The results produced by \mathbf{A}_1 are with lower p_e compared to the results produced by \mathbf{A}_0 . The reduction is .05, relatively to the result produced by the map \mathbf{A}_0 . Higher aCFP modulation results in lower p_e , as shown in Table 3 at modulation level 60 the p_e is lower than the one at modulation level 10.

In summary, the modulation distortion and the probability of bit error depends on the ability of the linear map to produce robust features and the properties of the linear map, related to the optimal linear modulation. The results produced by the proposed linear modulation show that small p_e is achievable under different and severe signal processing distortions, however at cost of introducing modulation distortion.

5. CONCLUSION

This paper proposed a generalized aCFP problem formulation, a reduction of the aCFP with linear modulation to a constrained projection problem and a closed form solution. The linear modulation in local context was addressed using a constrained projection problem where a convex constraint on the properties of the resulting local descriptor was introduced. The computer simulation using local image patches, extracted from publicly available data set was provided and the advantages under the distortions AWGN, lossy JPEG compression and projective geometrical transform were demonstrated.

6. APPENDIX A

By definition, problem (2) implies that $\mathbf{x} = \mathbf{x}_o + \mathbf{x}_e$ where \mathbf{x}_e is the error term. A multiplication from left side by the matrix \mathbf{A} results in $\mathbf{A}\mathbf{x} = \mathbf{A}\mathbf{x}_o + \mathbf{A}\mathbf{x}_e$. This expression in term of the error is: $\mathbf{A}\mathbf{x}_e = \mathbf{A}\mathbf{x} - \mathbf{A}\mathbf{x}_o$.

aCFP			
		p_e	
mL		10	60
DWR		51	28
	0dB	.15	.11
AWGN	5dB	.11	.05
	10dB	.08	.01
	20dB	.02	0
mL		10	30
DWR		51	42
	0	.02	0
QF	5	.01	0
	10	0	0
mL		10	60
DWR		51	28
Projective	QF=5	.05	.03

Table 2. The DWR and p_e using varying aCFP modulation under under varying AWGN noise, varying JPEG compression levels and projective transformation with QF level of 5.

Define $\mathbf{t}_s = \mathbf{A}\mathbf{x}$ and $\mathbf{t}_o = \mathbf{A}\mathbf{x}_o$, the closest vector (in Euclidean sense) \mathbf{t}_s to \mathbf{t}_o is a solution of the problem:

$$\hat{\mathbf{t}}_s = \underset{\mathbf{t}_s}{\operatorname{argmin}} \frac{1}{2} (\mathbf{t}_o - \mathbf{t}_s)^T (\mathbf{t}_o - \mathbf{t}_s) \quad (3)$$

subject to

$$|\mathbf{t}_s| \geq_e \tau \mathbf{1}.$$

Theorem 2: The optimal solution to (3) is: $\hat{\mathbf{t}}_s = \operatorname{sign}(\mathbf{t}_o) \odot \max\{|\mathbf{t}_o|, \tau \mathbf{1}\}$.

Proof: See Appendix B.

Replace the solution of (3) in the error term, use sign magnitude decomposition of $\mathbf{A}\mathbf{x}_o$ and reorder:

$$\begin{aligned} \mathbf{A}\mathbf{x}_e &= \operatorname{sign}(\mathbf{A}\mathbf{x}_o) \odot \max\{|\mathbf{A}\mathbf{x}_o|, \tau \mathbf{1}\} - \mathbf{A}\mathbf{x}_o \\ &= \operatorname{sign}(\mathbf{A}\mathbf{x}_o) \odot \max\{\tau \mathbf{1} - |\mathbf{A}\mathbf{x}_o|, \mathbf{0}\} = \mathbf{t}_e, \end{aligned} \quad (4)$$

if the pseudo inverse \mathbf{A}^\dagger of \mathbf{A} exists than the closed form solution to (2) is :

$$\mathbf{x} = \mathbf{x}_o + \mathbf{A}^\dagger \mathbf{t}_e. \quad (5)$$

7. APENDIX B

An equivalent problem representation to (3) is:

$$\hat{\mathbf{t}}_s = \underset{\mathbf{t}_s}{\operatorname{argmin}} \frac{1}{2} (\mathbf{t}_o - \mathbf{t}_s)^T (\mathbf{t}_o - \mathbf{t}_s) \quad (6)$$

subject to

$$\begin{aligned} \mathbf{t}_s \odot \mathcal{I}(\mathbf{t}_o \geq 0) &\geq_e \tau \mathbf{1} \odot \mathcal{I}(\mathbf{t}_o \geq 0) \\ \mathbf{t}_s \odot \mathcal{I}(\mathbf{t}_o < 0) &\leq_e -\tau \mathbf{1} \odot \mathcal{I}(\mathbf{t}_o < 0). \end{aligned}$$

Let $\lambda_1 = \lambda_{1,+} \odot \mathcal{I}(\mathbf{t}_o \geq 0)$ and $\lambda_2 = \lambda_{2,-} \odot \mathcal{I}(\mathbf{t}_o < 0)$ then the Lagrangian for (6) is:

$$\begin{aligned} l(\mathbf{t}_s, \lambda_1, \lambda_2) &= \frac{1}{2} (\mathbf{t}_o - \mathbf{t}_s)^T (\mathbf{t}_o - \mathbf{t}_s) \\ &\quad - \lambda_1^T (-\mathbf{t}_s + \tau \mathbf{1}) - \lambda_2^T (\mathbf{t}_s + \tau \mathbf{1}). \end{aligned} \quad (7)$$

By setting the first order derivative of (7) with respect to \mathbf{t}_s , the optimal $\hat{\mathbf{t}}_s$ can be expressed it terms of the optimal dual variables $\hat{\lambda}_1$ and $\hat{\lambda}_2$, and this expression is:

$$\hat{\mathbf{t}}_s = \mathbf{t}_o + \hat{\lambda}_1 - \hat{\lambda}_2. \quad (8)$$

Substituting (8) in (6), we have the dual problem:

$$\begin{aligned} \{\hat{\lambda}_1, \hat{\lambda}_2\} &= \underset{\lambda_1, \lambda_2}{\operatorname{argmax}} - \frac{1}{2} (-\lambda_1 + \lambda_2)^T (-\lambda_1 + \lambda_2) - \\ &\quad \lambda_1^T (-\mathbf{t}_o + \tau \mathbf{1}) - \lambda_2^T (\mathbf{t}_o + \tau \mathbf{1}) \\ &\text{subject to} \\ &\lambda_1 \geq_e \mathbf{0} \\ &\lambda_2 \geq_e \mathbf{0}. \end{aligned} \quad (9)$$

The optimal $\hat{\lambda}_1$ and $\hat{\lambda}_2$ must satisfy $\hat{\lambda}_1 \odot \hat{\lambda}_2 = \mathbf{0}$, implies that $\forall i$ if $\lambda_1(i) = 0$ then $\lambda_2(i) = 0$ or $\lambda_2(i) \neq 0$ and conversely, under the constraints $\lambda_1(i) \geq 0$ and $\lambda_2(i) \geq 0$. Therefore (9) can be splinted and solved independently for λ_1 and λ_2 under the constraint $\lambda_1 \odot \lambda_2 = \mathbf{0}$. The two sub-problems are:

$$\begin{aligned} \mathbf{P}^+ : \hat{\lambda}_1 &= \underset{\lambda_1}{\operatorname{argmax}} - \frac{1}{2} \lambda_1^T \lambda_1 - \lambda_1^T (-\mathbf{t}_o + \tau \mathbf{1}) \\ &\text{subject to} \\ &\lambda_1 \geq_e \mathbf{0}. \end{aligned} \quad (10)$$

$$\begin{aligned} \mathbf{P}^- : \hat{\lambda}_2 &= \underset{\lambda_2}{\operatorname{argmax}} - \frac{1}{2} \lambda_2^T \lambda_2 - \lambda_2^T (\mathbf{t}_o + \tau \mathbf{1}) \\ &\text{subject to} \\ &\lambda_2 \geq_e \mathbf{0}. \end{aligned} \quad (11)$$

By taking the first order derivative in (10) and (11) with respect to λ_1 and λ_2 respectively and equalling to zero, the optimal solution for (9) that satisfy the constraint $\hat{\lambda}_1 \odot \hat{\lambda}_2 = \mathbf{0}$, $\hat{\lambda}_2 \geq_e \mathbf{0}$ and $\hat{\lambda}_1 \geq_e \mathbf{0}$ is:

$$\begin{aligned} \hat{\lambda}_1 &= \mathcal{I}(\mathbf{t}_o \geq \mathbf{0}) \odot \max\{\tau \mathbf{1} - \mathbf{t}_o, \mathbf{0}\} \\ \hat{\lambda}_2 &= \mathcal{I}(\mathbf{t}_o < \mathbf{0}) \odot \max\{\tau \mathbf{1} + \mathbf{t}_o, \mathbf{0}\}, \end{aligned} \quad (12)$$

substituting (12) back in (8), reordering and using sign magnitude decomposition of \mathbf{t}_o we have:

$$\hat{\mathbf{t}}_s = \mathbf{t}_o + \hat{\lambda}_1 - \hat{\lambda}_2 = \operatorname{sign}(\mathbf{t}_o) \max\{|\mathbf{t}_o|, \tau \mathbf{1}\},$$

that gives **Theorem 2**.

8. REFERENCES

- [1] S.Voloshynovskiy, F. Farhadzadeh, O. Koval, and T. Holotyak, "Active content fingerprinting: a marriage of digital watermarking and content fingerprinting," in *Proceedings of IEEE International Workshop on Information Forensics and Security*, Tenerife, Spain, December 2–5 2012.
- [2] F. Farhadzadeh, F. Willems, and S.Voloshynovskiy, "Information-theoretical limits of active content fingerprinting in content-based identification systems," in *Proceedings of IEEE International Workshop on Information Forensics and Security*, Rome, Italy, November 16–19 2015.
- [3] F. Farhadzadeh and S. Voloshynovskiy, "Active content fingerprinting," *Information Forensics and Security, IEEE Transactions on*, vol. 9, no. 6, pp. 905–920, June 2014.
- [4] F. Farhadzadeh, S. Voloshynovskiy, T. Holotyak, and F. Beekhof, "Active content fingerprinting: Shrinkage and lattice based modulations," in *Acoustics, Speech and Signal Processing (ICASSP), 2013 IEEE International Conference on*, 2013, pp. 3073–3077.
- [5] David G. Lowe, "Distinctive image features from scale-invariant keypoints," *International Journal of Computer Vision*, vol. 60, pp. 91–110, 2004.
- [6] M. Calonder, V. Lepetit, M. Ozuysal, T. Trzcinski, C. Strecha, and P. Fua, "BRIEF: Computing a Local Binary Descriptor Very Fast," *IEEE Transactions on Pattern Analysis and Machine Intelligence*, vol. 34, no. 7, pp. 1281–1298, 2012.
- [7] S Leutenegger, M Chli, and RY Siegwart, "Brisk: Binary robust invariant scalable keypoints," 2011, pp. 2548–2555.
- [8] Ethan Rublee, Vincent Rabaud, Kurt Konolige, and Gary Bradski, "Orb: an efficient alternative to sift or surf," in *Computer Vision (ICCV), 2011 IEEE International Conference on*. IEEE, 2011, pp. 2564–2571.
- [9] Matti Pietikainen, Abdenour Hadid, Guoying Zhao, and Timo Ahonen, *Computer Vision Using Local Binary Patterns*, Computational imaging and vision. Springer Verlag, London, 2011.
- [10] Gerald Schaefer and Michal Stich, "Ucid: an uncompressed color image database," in *Electronic Imaging 2004*. International Society for Optics and Photonics, 2003, pp. 472–480.